Hyperpolarized 13C Urea Relaxation Mechanism Reveals Renal Changes in Diabetic Nephropathy

Laustsen, Christoffer; Stokholm Nørlinger, Thomas; Christoffer Hansen, David; Qi, Haiyun; Nielsen, Per Mose; Bonde Bertelsen, Lotte; Ardenkjær-Larsen, Jan Henrik; Stødkilde Jørgensen, Hans

Published in:
Magnetic Resonance in Medicine

Link to article, DOI:
10.1002/mrm.26036

Publication date:
2016

Document Version
Publisher's PDF, also known as Version of record

RAPID COMMUNICATION

Magnetic Resonance in Medicine 00:00–00 (2015)

Hyperpolarized ^{13}C Urea Relaxation Mechanism Reveals Renal Changes in Diabetic Nephropathy

Christoffer Laustsen,[1]* Thomas Stokholm Nørlinger,[1] David Christoffer Hansen,[1] Haiyun Qi,[1] Per Mose Nielsen,[1] Lotte Bonde Bertelsen,[1] Jan Henrik Ardenkjaer-Larsen,[2,3] and Hans Stødkilde Jørgensen[1]

Purpose: Our aim was to assess a novel ^{13}C radial fast spin echo golden ratio single shot method for interrogating early renal changes in the diabetic kidney, using hyperpolarized (HP) [^{13}C,^{15}N$_2$]urea as a T_2 relaxation based contrast bio-probe.
Methods: A novel HP ^{13}C MR contrast experiment was conducted in a group of streptozotocin type-1 diabetic rat model and age matched controls.
Results: A significantly different relaxation time ($P = 0.004$) was found in the diabetic kidney (0.49 ± 0.03 s) compared with the controls (0.64 ± 0.02 s) and secondly, a strong correlation between the blood oxygen saturation level and the relaxation times were observed in the healthy controls.
Conclusion: HP [^{13}C,^{15}N$_2$]urea apparent T_2 mapping may be a useful for interrogating local renal pO_2 status and renal tissue alterations. **Magn Reson Med 000:000–000, 2015.**

Key words: MRI; type 1 diabetes; kidney; renal metabolism; hyperpolarization

INTRODUCTION

The development of early diabetic nephropathy (DN) is characterized by several renal metabolic and structural changes including glomerular hyperfiltration, glomerular and renal hypertrophy and increased urinary albumin excretion (1). In contrast, overt diabetic nephropathy is characterized by a decline in renal function, decreasing creatinine clearance, glomerulosclerosis, and tubulointerstial fibrosis. Albeit several MRI methods show great promise, lengthy acquisition times reduce the clinical impact of the methods (2). Alternatively, dissolution dynamic nuclear polarization ^{13}C-labeled pyruvate was recently introduced as a possible endogenous marker to identify renal metabolic changes in diabetic rats (3–5) within seconds after the bolus injection of the bio-probe. Interestingly, the pyruvate-to-lactate conversion is seen to correlate with the progression of DN, in parallel to the structural and microvasculature changes. Additionally, several non-metabolic ^{13}C-labeled hyperpolarized agents such as urea and HP001 (bis-1,1-(hydroxymethyl)-[1-(13)C]cyclopropane-d(8)) have unique abilities for renal angiographic and perfusion studies (6–9) and could, therefore, be used for examination of renal changes associated with DN. MR renal examination without use of gadolinium has gained increasing interest for patients with renal insufficiency and ^{13}C-labeled pyruvate injections can be done without any risk of nephrogenic systemic fibrosis.

In standard proton MRI the contrast mechanism is coupled to signal relaxation. This is in contrast to hyperpolarized MR, where the signal intensity is the determinant. Hyperpolarized pulse sequences are designed to use the magnetization efficiently. T_2 mapping by means of the radial fast spin echo (FSE) train has previously been shown to yield accurate T_2 values (10) for thermal ^{1}H imaging. Mapping of the transverse ^{1}H relaxation times T_2 has been shown to accurately characterize the altered composition of the renal tissue following acute kidney injury (11), while quantitative evaluation of oxygenation in venous vessels using T_2-relaxation-under-spin-tagging (TRUST) MRI has been shown to correlate with the increased oxygen consumption in the brain and has been proposed as a novel method for renal oxygen monitoring (2). We, therefore, state the hypothesis, that early renal changes are observable with hyperpolarized urea through the apparent transverse relaxation rate. The cortico-medulla urea gradient introduces different local milieus for the urea molecules and hence introduces contrast mechanisms. The present study addresses the potential for using T_2 relaxation mechanisms of, hyperpolarized urea, a metabolic end-product, to interrogate both oxygen availability and the macroscopic renal changes seen in early diabetes.

[1]MR Research Centre, Department of Clinical Medicine, Aarhus University, Aarhus, Denmark.
[2]GE Healthcare, Broendby, Denmark.
[3]Department of Electrical Engineering, Technical University of Denmark, Kgs Lyngby, Denmark.
Grant sponsor: The Danish Research Council; Grant sponsor: The Danish Kidney Foundation; Grant sponsor: Helen and Ejnar Bjørnows Foundation; Grant sponsor: the Strategic Research Council.
*Correspondence to: Christoffer Laustsen, Ph.D., Palle Juul-Jensens Boulevard 99, 8200 Aarhus N, Denmark. E-mail: cl@clin.au.dk
Received 1 September 2015; revised 1 October 2015; accepted 15 October 2015
DOI 10.1002/mrm.26036
Published online 00 Month 2015 in Wiley Online Library (wileyonlinelibrary.com).

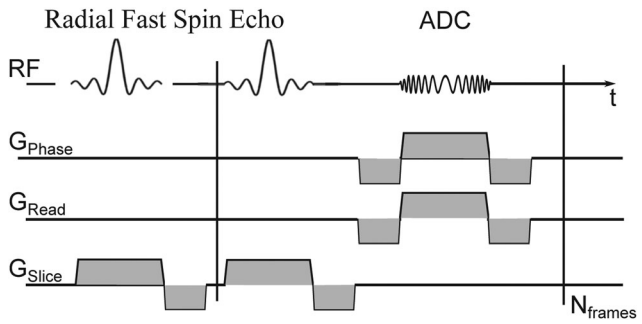

FIG. 1. A pulse sequence illustration of the radial 2D FSE sequence, with slice selective excitation and refocusing pulses. The radial angle scheme used was the golden ratio of 111.25° ensuring high temporal k-space coverage allowing time resolved images to be reconstructed.

METHODS

A single shot radial FSE sequence (Fig. 1), with golden ratio encoding was implemented on a 9.4 Tesla (T) with VnmrJ 4.0 (Agilent, Santa Clara CA) for in vivo relaxation mapping. It has previously been shown that the 180° refocusing pulses found in FSE type sequences is superior to the lower flip angle refocusing often used in balanced steady state thermal ^{1}H imaging sequences (7). The radial ordering scheme golden ratio (111.25°) have been used for free breathing MR and recently have shown excellent abilities for ^{3}He gas MR of the lung (12), where the transient longitudinal T_1 relaxation yields similar quantitative difficulties as seen in 13C HP MR.

Twelve 9-week-old female Wistar rats weighing 208.6 ± 7.5 g, were included in this study. The rats were randomly grouped in a diabetic (N = 6) and a healthy control group (N = 6). Two rats were excluded from the study, due to erroneous or incomplete data sampling resulting in n = 5 in each group. The rats were kept in cages with a 12:12-h light:dark cycle, a temperature of 21 ± 2°C and a humidity of 55 ± 5% and all animals had free access to water and standard chow throughout the study. Diabetes was induced by an i.v. injection of freshly prepared streptozotocin (STZ; 55 mg/kg body weight; Sigma-Aldrich, Brøndby, DK) dissolved in 0.3 mL of 10 mmol/L cold sodium citrate buffer (pH 4.5). Blood glucose was measured in tail-capillary blood with a ContourXT blood glucose meter (Bayer Diabetes Care, Copenhagen, Denmark). Rats were considered diabetic when the blood glucose levels exceeded 15 mmol/L at 48 h after injection of STZ. Eight to 10 days after induction of diabetes, the tail vein was catheterized for hyperpolarized [^{13}C,^{15}N$_2$]urea administration. The animals were anesthetized with 3% sevoflurane in 2 L/min air. Subsequently, animals were positioned in a preclinical 9.4T MRI for functional hyperpolarized imaging. The temperature was maintained at 35°C and respiration and peripheral capillary oxygen saturation (SpO_2) level was monitored throughout the experiment with a MR compatible monitoring system (SA Instruments, Inc, Stony Brook, NY). ^{1}H T_2-weighted FSE coronal and axial scans were acquired [repetition time/echo time (TR/TE) 3 s/4 ms, field of view (FOV) 70 × 70, matrix 192 × 192] as a scout and a single shot ^{13}C radial FSE sequence (FOV 60 × 60 mm^2, matrix 64 × 512, sw = 50 kHz, TR/TE 2.4 s/4.6 ms, 1 axial 10 mm slice) covering both kidneys was performed. After the MRI section, a 5- to 7-mL blood sample was collected from the aortic bifurcation to ethylenediaminetetraacetic acid coated tubes for determination of plasma electrolytes and osmolality. The study complied with the guidelines for use and care of laboratory animals and was approved by the Danish Inspectorate of Animal Experiments (2012-15-2934-00581). A standard solution state thermal NMR (Carr-Purcell Meiboom-Gill) CPMG experiment with hard pulses, with an inter-pulse delay τ of 3 ms, a TR of 105 s and varying TEs of 2.5, 5, 10, 20, 40, 80 s, respectively, was run to examine the relaxation behavior of [^{13}C,^{15}N]urea at 9.4T.

Hyperpolarization

A total of 200 μL of [^{13}C,^{15}N$_2$]urea (Sigma-Aldrich, Brøndby, DK), glycerol (Sigma-Aldrich,Brøndby, DK), AH111501 (GE Healthcare, Brøndby, DK) (6.4 M concentration) mixed weight ratio (0.30:0.68:0.02) was polarized in a 5T SPINLab (GE Healthcare, Brøndby, DK) to a reproducible polarization of more than 30%.

MRI Analysis

Data were converted to ISMRMRD format by means of an open source MATLAB (MathWorks, Natick, MA) converter (www.mr.au.dk/software) and reconstructed in the open-source software GADGETRON (13) with a time resolution of eight radial spokes per image. Reconstruction was performed on the graphics processing unit, where the non-Cartesian Fourier transform was inverted using an iterative solver with total variation regularization was added, to suppress noise (14). The images were then transferred to Osirix (15), where region of interest (ROI) analysis was performed; separating the renal segments into a cortex, medulla, and papilla segments. A single exponential fit was found to accurately fit the different segments individually in MATLAB with a single exponential fit (Fig. 2).

Statistics

Normality was assessed with quantile plots. $P < 0.05$ (*) were considered statistically significant. A two-way

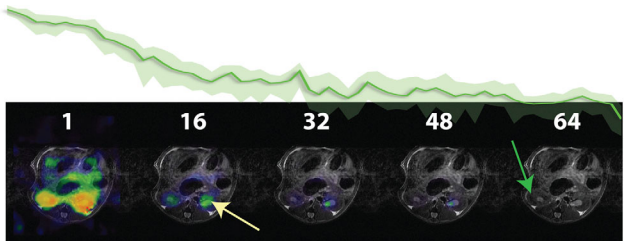

FIG. 2. A representative image series (image 1 - image 64) of a ^{1}H T_2 weighted FSE axial slice overlaid hyperpolarized [^{13}C,^{15}N] urea with each image constructed by eight radial spokes. The images are normalized to the first image of the series (all images are shown logarithmic scaled) and the green line (solid) is the ROI time curve (transparent illustrates SD) from the renal cortex (green arrow). An intra-renal difference in signal is observable after 16 s (yellow arrow) showing elevated signal in the medulla, while no or little signal is observable after 512 refocusing pulses (image 64).

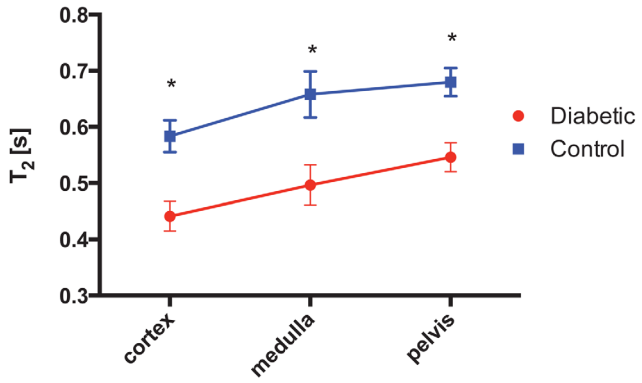

FIG. 3. T_2 relaxation times as a function of kidney ROI segments, showing an overall decrease from the kidney pelvis medulla region toward the cortex in both groups, however, a significant decrease in T_2 values was found in the diabetic kidney compared with the controls (mean±SEM).

analysis of variance (ANOVA) was used for statistical analysis of the T_2 relaxation times across the kidney regions in GraphPad, Prism (GraphPad Software, Inc. La Jolla, CA). Linear regression was used to assess the correlation between pO_2 and T_2 values. Data on animal body and kidney weight and blood glucose were analyzed with a two-tailed student t-test with equal variance.

RESULTS

All rats that received STZ developed sustained hyperglycemia over 48 h. On the day of the scan, the mean body weight of the diabetic rats was 222.4 ± 3.6 g and of the healthy controls 221.3 ± 2.7 g ($P = 0.81$). However, the weight of the diabetic kidney (0.960 ± 0.025 g) was significantly higher compared with the controls (0.800 ± 0.032; $P = 0.0039$). The change in kidney weight was concomitant with an significant increased blood glucose level in the diabetic animals of 24.71 ± 0.91 mmol/L compared with the controls 6.97 ± 0.39 mmol/L ($P < 0.0001$). A significant intra-renal difference in T_2 relaxation times as a function of kidney region was found ($P < 0.0001$) between the two groups (Fig. 3), as well as an overall significant reduction in the T_2 relaxation times in the diabetic group compared with the controls ($P = 0.011$). To examine the effect of oxygen availability in the investigations the correlation between the mean T_2 relaxation time and the SpO_2 saturation was investigated. It revealed a significant difference in elevation ($P = 0.0045$) between the control group ($R^2 = 0.98$; $P = 0.016$) and the diabetic group ($R^2 = 0.0003$; $P = 0.98$), as the diabetic group shows no correlation with SpO_2 (Fig. 4). Thermal phantom 1D CPMG NMR experiments confirmed the existence of a single exponential T_2 decay of 6 s in solution at 9.4T.

DISCUSSION

The main finding was a significant difference in the T_2 relaxation time between the diabetic and healthy control. A significant correlation between SpO_2 and hyperpolarized ^{13}C urea T_2 relaxation was found in the healthy group. It, therefore, seems plausible to attribute the difference in T_2 relaxation between the diabetic and healthy control group to a difference in local pO_2 (hypoxia, increased deoxyhemoglobin), at least in part. Most likely, T_2 is also affected by changes in other tissue properties such as protein content. The decrease in T_2 might originate from either structural changes (hypotrophy and fibrosis) or increased oxygen consumption or both; however, further studies are needed to elucidate the origin of this relaxation mechanism. The difference between the response in the healthy control and the diabetic groups may originate from the increased oxygen consumption observed in the diabetic kidney leading to hypoxia, thus directly linking diabetes with the development of chronic kidney disease (16–18).

Of interest, it has been shown that an increased concentration of urea in the blood is directly coupled with insulin resistances and oxidative stress (19,20) creating an over stimulated situation in the diabetic kidney compared with the healthy control. The study indicates a potential for interrogating SpO_2 directly with hyperpolarized bio-probes having benefit of being transient signals originating from the bio-probe itself and thus a positive contrast mechanism directly coupled to the bio-probes local milieu. The single shot nature of this current method provide beneficial speed, while the background less hyperpolarization ensures robustness in the quantification process, compared with TRUST or BOLD. Dual-isotopically enriched [^{13}C,$^{15}N_2$]urea has been shown to significantly increase T_2 in vivo compared with [^{13}C,$^{14}N_2$]urea, thus improving the obtainable signal-to-noise ratio (21). The T_2 relaxation times found here do not correspond to previous findings at 3T that showed bi-exponential and longer T_2 relaxation times (21), however, does agree with findings of similar sized molecules at 9.4T finding T_2 relaxation times in the range 0.1–0.6 s (22,23). This may originate from higher magnetic field and the continuous crushing of inflowing spins by gradients and imperfect refocusing in this sequence, due to the use of slice selective excitation and refocusing in contrast to spatial non selective pulses in Reed et al (21). Hence, a lower overall T_2 will be found with a single component.

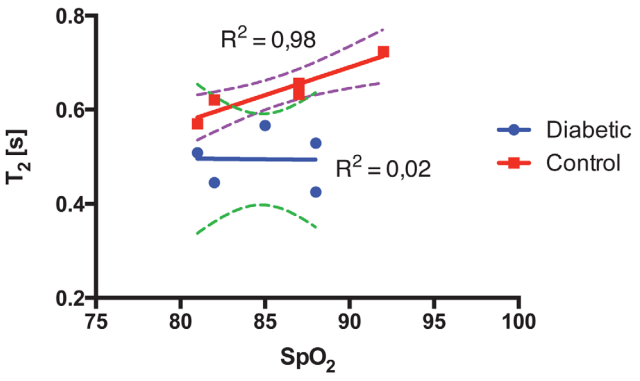

FIG. 4. A significant correlation between the healthy renal controls T_2 values and SpO_2 was observed, while no correlation was found in the diabetic kidneys. The cyan and green stippled lines illustrate the 95% confidence intervals for the interactions.

A limitation of the current experimental setup was the use of 10 mm slices thickness (mean intensity profile view), allowing partial volume effects, smearing the ROI signals, further studies are needed for extending the method to three-dimensional. A potential alternative to urea is hyperpolarized water, which would increase the T_2 relaxation and hence improve the sensitivity of the proposed method (24). The method shows the ability to get high resolution and high temporal resolution imaging of hyperpolarized compounds, allowing determination of apparent T_2 relaxation values in vivo. Additionally, the radial acquisition ensures motion robustness for high temporal changes such as respiration. Our results highlight the potential for using HP relaxation contrast MR for probing cellular and macroscopic changes associated with renal disease, with a significant difference between the diabetic and control kidneys.

ACKNOWLEDGMENTS

Henrik Vestergaard Nielsen is acknowledged for his expert laboratory assistance.

REFERENCES

1. Schrijvers BF, De Vriese AS, Flyvbjerg A. From hyperglycemia to diabetic kidney disease: the role of metabolic, hemodynamic, intracellular factors and growth factors/cytokines. Endocr Rev 2004;25: 971–1010.
2. Liss P, Cox EF, Eckerbom P, Francis ST. Imaging of intrarenal haemodynamics and oxygen metabolism. Clin Exp Pharmacol Physiol 2013; 40:158–167.
3. Laustsen C, Lipso K, Ostergaard JA, Norregaard R, Flyvbjerg A, Pedersen M, Palm F, Ardenkjær-Larsen JH. Insufficient insulin administration to diabetic rats increases substrate utilization and maintains lactate production in the kidney. Physiol Rep 2014;2: e12233
4. Laustsen C, Lycke S, Palm F, Ostergaard JA, Bibby BM, Norregaard R, Flyvbjerg A, Pedersen M, Palm F, Ardenkjær-Larsen JH. High altitude may alter oxygen availability and renal metabolism in diabetics as measured by hyperpolarized [1-13C]pyruvate magnetic resonance imaging. Kidney Int 2014;86:67–74
5. Laustsen C, Østergaard JA, Lauritzen MH, Nørregaard R, Bowen S, Søgaard LV, Flyvbjerg A, Pedersen M, Ardenkjaer-Larsen JH. Assessment of early diabetic renal changes with hyperpolarized [1-13C]pyruvate. Diabetes Metab Res Rev 2013;29:125–129.
6. Johansson E, Olsson LE, Månsson S, Petersson JS, Golman K, Ståhlberg F, Wirestam R. Perfusion assessment with bolus differentiation: a technique applicable to hyperpolarized tracers. Magn Reson Med 2004;52:1043–1051.
7. Svensson J, Månsson S, Johansson E, Petersson JS, Olsson LE. Hyperpolarized 13C MR angiography using trueFISP. Magn Reson Med 2003;50:256–262.
8. von Morze C, Bok RA, Sands JM, Kurhanewicz J, Vigneron DB. Monitoring urea transport in rat kidney in vivo using hyperpolarized 13C magnetic resonance imaging. Am J Physiol Renal Physiol 2012;302: F1658–F1662
9. Johansson E, Månsson S, Wirestam R, Svensson J, Petersson JS, Golman K, Ståhlberg F. Cerebral perfusion assessment by bolus tracking using hyperpolarized 13C. Magn Reson Med 2004;51:464–472.
10. Altbach MI, Outwater EK, Trouard TP, Krupinski EA, Theilmann RJ, Stopeck AT, Kono M, Gmitro AF. Radial fast spin-echo method for T2-weighted imaging and T2 mapping of the liver. J Magn Reson Imaging 2002;16:179–189.
11. Hueper K, Rong S, Gutberlet M, Hartung D, Mengel M, Lu X, Haller H, Wacker F, Meier M, Gueler F. T2 relaxation time and apparent diffusion coefficient for noninvasive assessment of renal pathology after acute kidney injury in mice: comparison with histopathology. Invest Radiol 2013;48:834–842.
12. Marshall H, Ajraoui S, Deppe MH, Parra-Robles J, Wild JM. K-space filter deconvolution and flip angle self-calibration in 2D radial hyperpolarised 3He lung MRI. NMR Biomed 2012;25:389–399.
13. Hansen MS, Sorensen TS. Gadgetron: an open source framework for medical image reconstruction. Magn Reson Med 2013;69:1768–1776.
14. Goldstein T, Osher S. The Split Bregman Method for L1-regularized problems. Siam J Imaging Sci 2009;2:323–343.
15. Rosset A, Spadola L, Ratib O. OsiriX: an open-source software for navigating in multidimensional DICOM images. J Digit Imaging 2004; 17:205–216.
16. Palm F, Hansell P, Ronquist G, Waldenstrom A, Liss P, Carlsson PO. Polyol-pathway-dependent disturbances in renal medullary metabolism in experimental insulin-deficient diabetes mellitus in rats. Diabetologia 2004;47:1223–1231.
17. Friederich-Persson M, Thorn E, Hansell P, Nangaku M, Levin M, Palm F. Kidney hypoxia, attributable to increased oxygen consumption, induces nephropathy independently of hyperglycemia and oxidative stress. Hypertension 2013;62:914–919.
18. Palm F, Nordquist L. Renal tubulointerstitial hypoxia: cause and consequence of kidney dysfunction. Clin Exp Pharmacol Physiol 2011; 38:474–480.
19. D'Apolito M, Du X, Zong H, et al. Urea-induced ROS generation causes insulin resistance in mice with chronic renal failure. J Clin Invest 2010;120:203–213.
20. Palm F, Nangaku M, Fasching A, et al. Uremia induces abnormal oxygen consumption in tubules and aggravates chronic hypoxia of the kidney via oxidative stress. American journal of physiology Renal Physiol 2010;299:F380–F386.
21. Reed GD, von Morze C, Bok R, Koelsch BL, Van Criekinge M, Smith KJ, Hong Shang, Larson PE, Kurhanewicz J, Vigneron DB. High resolution (13)C MRI with hyperpolarized urea: in vivo T(2) mapping and (15)N labeling effects. IEEE Trans Med Imaging 2014;33:362–371.
22. Kennedy BW, Kettunen MI, Hu DE, Brindle KM. Probing lactate dehydrogenase activity in tumors by measuring hydrogen/deuterium exchange in hyperpolarized l-[1-(13)C,U-(2)H]lactate. J Am Chem Soc 2012;134:4969–4977.
23. Kettunen MI, Kennedy BW, Hu DE, Brindle KM. Spin echo measurements of the extravasation and tumor cell uptake of hyperpolarized [1-(13) C]lactate and [1-(13) C]pyruvate. Magn Reson Med 2013;70: 1200–1209.
24. Ardenkjaer-Larsen JH, Laustsen C, Bowen S, Rizi R. Hyperpolarized H_2O MR angiography. Magn Reson Med 2014;71:50–56.